

Ground-state phases of polarized deuterium species

R. M. Panoff

Department of Physics, Kansas State University, Manhattan, Kansas 66506

J. W. Clark*

Theoretical Division and Center for Nonlinear Studies, MSB62, Los Alamos National Laboratory, Los Alamos, New Mexico 87545

(Received 23 March 1987)

Microscopic prediction of the ground-state phase of electron-spin-aligned bulk atomic deuterium ($D\downarrow$) is attempted, based on the variational Monte Carlo method. The accurate pair potential of Kolos and Wolniewicz is assumed, and three versions of $D\downarrow$ are considered, which, respectively, involve one, two, and three equally occupied nuclear spin states. The most definitive results on the zero-temperature equations of state of these systems are obtained with optimized ground-state trial wave functions incorporating Jastrow pair correlations, triplet correlations, and momentum-dependent backflow effects. The species $D\downarrow_3$ is bound already at the pure Jastrow level, while the energy expectation value of $D\downarrow_2$ dips below zero upon supplementing the Jastrow description by triplets and momentum-dependent backflow. The variational energy of $D\downarrow_1$ remains positive under all current refinements of the ground-state trial function. We conclude that the systems $D\downarrow_3$ and $D\downarrow_2$, if they could be manufactured and stabilized at relevant densities, would be Fermi liquids at sufficiently low temperature; on the other hand, it is likely that $D\downarrow_1$ would remain gaseous down to absolute zero.

I. INTRODUCTION

An interesting question in the theory of quantum fluids (though still a hypothetical one) concerns the nature of the ground-state phases of various species of bulk electron-spin-aligned atomic deuterium $D\downarrow$, at zero temperature under vanishing external pressure. The three species commonly considered,^{1,2} designated $D\downarrow_1$, $D\downarrow_2$, and $D\downarrow_3$, have respectively one, two, and three accessible nuclear spin states. Assuming equal occupation of the available spin states in the latter two cases, the three realizations of $D\downarrow$ are regarded as spin-saturated systems of elementary fermions with respective level degeneracies $\nu=1, 2$, and 3 . van der Waals forces are assumed to act between the constituent atoms. However, the composite nature of the deuterium atoms is suppressed, and, in particular, hyperfine interactions are disregarded; in that sense the problem is posed in a somewhat idealized form.

One may liken $D\downarrow_1$ to fully polarized bulk ^3He , having all its nuclear spins aligned; and $D\downarrow_2$ to ordinary, unpolarized ^3He . On the other hand, at densities near equilibrium, the deuterium systems are not nearly so strongly coupled as liquid ^3He ; hence, their quantitative microscopic treatment is generally not so demanding. Indeed, for many purposes a Jastrow wave function and integral-equation evaluation of the corresponding distribution functions provides a reasonable description of the ground states of these systems. However, in the determination of the ground-state phase of the $D\downarrow$ systems—gas or self-bound liquid—we face an exception requiring more delicate treatment, since the kinetic-potential balance in the ground state of $D\downarrow$, near the finite-density minimum of the curve of energy versus density, is so close that errors in any conventional many-body method (e.g., Jastrow-

Fermi-hypernetted-chain^{3,4}) obscure the sign of the estimated energy. To achieve the necessary refinement in accuracy, appeal must be made to Monte Carlo (MC) sampling algorithms and variational Monte Carlo (VMC) calculations. A few years ago, such a calculation⁵ ruled definitively in favor of a liquid rather than a gaseous ground state for $D\downarrow_3$. In fact, this system binds even with a Jastrow wave function. The aim of the current study is to clarify the situation for the other two systems. Comprehensive VMC results will be presented for all three values of ν , based on (a) parametrized and “optimal” Jastrow wave functions and on (b) more elaborate trial wave functions including state-independent (Jastrow) pair correlations, triplet correlations, and backflow. These results will be compared with the best available calculations from Fermi-hypernetted-chain (FHNC) theory² and from the method of correlated basis functions⁶ (CBF).

From the standpoint of many-body theory, the problem posed above is a particularly attractive one. We have here an example where the basic two-body interaction is very accurately known; it is reproduced with great precision by the theoretical $b^3\Sigma_u^+$ potential of Kolos and Wolniewicz⁷ (KW). On the other hand, the substance $D\downarrow$ has not yet been produced in quantities or at densities allowing an experimental resolution of its ground-state phase under relevant conditions. Indeed, it is hard to see how this might be accomplished with current technology, although progress is still being made on the stabilization and concentration of $\text{H}\downarrow$ (see, for example, Refs. 8–11). An opportunity is therefore open for many-body theory to contribute incisive qualitative determinations and accurate quantitative predictions of the properties of a fundamental class of Fermi fluids, without any hints from experiment.

Our principal findings are the following: While $D\downarrow_2$

remains unbound at the Jastrow level, the introduction of triplet and backflow correlations into the variational ansatz suffices to reduce the energy minimum below zero. Thus $D\downarrow_2$, like $D\downarrow_3$, has a liquid ground state. Triplet and backflow correlations have very little effect in $D\downarrow_1$ and do not bring the energy below $+0.2$ K for the particular trial forms assumed. From all indications, the ground state of this system—as expected for $\nu=1$ and not-so-strong coupling—is well represented by a Jastrow wave function. It appears very likely that $D\downarrow_1$, like the mass-1 isotopic form $H\downarrow$, remains gaseous down to absolute zero. Also as expected, triplet and backflow correlations are more important in $D\downarrow_3$ than in the other two species, and produce a significant relative reduction in the energy. The energy ordering is well established as $E(D\downarrow_1) > E(D\downarrow_2) > E(D\downarrow_3)$. Where meaningful comparisons can be made, these predictions are in accord with results obtained by CBF perturbation theory.⁶

In Sec. II we report new variational Monte Carlo calculations on the deuterium systems at the Jastrow level; these and other available MC data are used to assess the accuracy of various aspects of corresponding FHNC/C evaluations. In Sec. III the VMC treatment is extended to include triplet and backflow correlations, and implications for the equations of state of $D\downarrow_1$, $D\downarrow_2$, and $D\downarrow_3$ are discussed. Section IV presents some Monte Carlo results for the radial distribution function $g(r)$ and the one-body density matrix $n(r)$, assuming Jastrow correlations. Appendix A addresses some key technical aspects of the MC sampling procedure, and Appendix B sketches the MC evaluations of $g(r)$ and $n(r)$.

II. JASTROW GROUND-STATE ENERGY

A. Fermi-hypernetted-chain results

We first attempt to resolve the issue of the ground-state phase assumed by the various species of $D\downarrow$ purely within the Jastrow description. Thus we adopt a variational approach in which a ground-state trial function Ψ_{trial} of the N -fermion system is formed by correlating the ground state Φ_0 of the noninteracting Fermi sea by a product of pair functions f :

$$\Psi_{\text{trial}} = \Psi_0 = F\Phi_0, \quad (2.1)$$

with

$$F = F_J = \prod_{i < j} f(r_{ij}). \quad (2.2)$$

The pair-correlation function $f(r)$, and the corresponding pair “pseudopotential” $u(r) = -2 \ln f(r)$, should ideally be determined by functional minimization of the energy expectation value per particle

$$\langle H \rangle = N^{-1} \frac{\langle \Psi_0 | H | \Psi_0 \rangle}{\langle \Psi_0 | \Psi_0 \rangle}, \quad (2.3)$$

i.e., by solving the Euler equation

$$\frac{\delta \langle H \rangle}{\delta u(r)} = 0. \quad (2.4)$$

We consider three prescriptions for $f(r)$ which fulfill this ideal to a lesser or greater extent.

(a) The Schiff-Verlet¹² (SV) or McMillan¹³ choice

$$f_{\text{SV}}(r) = \exp\left[-\frac{1}{2}(b/r)^5\right], \quad (2.5)$$

the scale parameter b being fixed by minimization of a suitable approximation (namely, FHNC/C or Monte Carlo) to the Jastrow expectation value (2.3).

(b) A Pandharipande-Bethe¹⁴ (PB) function, the lowest solution of the two-body Schrödinger-like equation

$$\left[-\frac{\hbar^2}{m} \nabla^2 + v(r) - \lambda \right] f(r) = 0 \quad (2.6)$$

in the interval $0 \leq r \leq d$, subject to $rf(r) \rightarrow 0$ as $r \rightarrow 0$ and to the healing conditions $f(d) = 1$ and $f'(d) = 0$. The Lagrange multiplier λ is fixed by the constraints, and the healing distance d remains as a single trial parameter which, again, may be varied at each density to minimize a chosen approximation to the energy per particle.

(c) The determination of an optimal correlation function within the FHNC/C scheme. This is clearly the preferred option among those considered here; for details of its implementation, see Ref. 2.

Reference 2 reports extensive numerical data on the Jastrow energy of the three systems $D\downarrow_1$, $D\downarrow_2$, and $D\downarrow_3$, for each of the above pair-correlation functions: Schiff-Verlet (SV), Pandharipande-Bethe (PB), and optimal (opt). The FHNC/C approximation was applied to evaluate the energy expectation value, for which three different forms were used, corresponding to Clark-Westhaus (CW), Jackson-Feenberg (JF), and Pandharipande-Bethe (PB) treatments of the kinetic-energy operator.³

In the SV case, the parameter b of (2.5) was determined for $D\downarrow_3$ at each density by minimizing the Jackson-Feenberg expectation value $\langle H \rangle_{\text{JF}}$. For $\nu=1$ and 2 the values $b(\nu, \rho)$ given by Miller^{1,15} were adopted, after checking that they minimize, or nearly minimize, $\langle H \rangle_{\text{JF}}$ as approximated in the FHNC/C scheme. All relevant b choices are tabulated in Ref. 2. In the calculations based on the PB correlation function, the healing distance d was chosen by minimizing $\langle H \rangle_{\text{JF}}$ for each species of $D\downarrow$ in the vicinity of the finite-density energy minimum found with f_{SV} . For all three degeneracies, an optimal value $d = 2.2r_0$ was obtained, where r_0 is the radius of a sphere of unit density. This healing distance was used for all densities studied. Finally, in the calculations involving an optimal pair correlation function f_{opt} , the FHNC/C Euler equation was solved at each density for each ν value.

Comparison of the detailed FHNC numerical results for a given density and degeneracy shows very little lowering of the energy per particle upon going to a more refined (more elaborately optimized) wave function of Jastrow form. Extensive energy-minimization searches for the parameter b in f_{SV} , and also for the healing distance d in f_{PB} , affirm that the energy is, within reasonable limits, insensitive to the detailed structure of the pair correlations

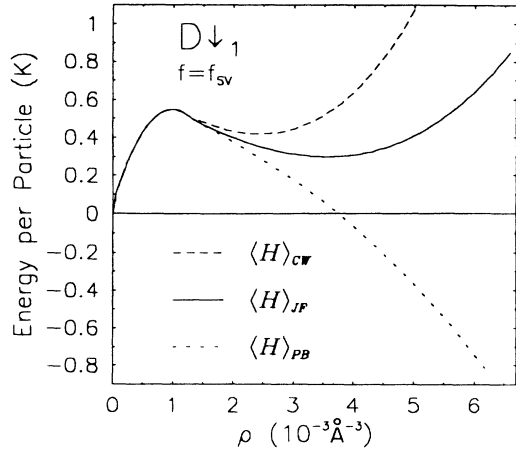


FIG. 1. Jastrow energy per particle versus density for the electron-spin-aligned deuterium system $D\downarrow_1$, based on the Kolos-Wolniewicz potential and the Schiff-Verlet correlation function $f_{SV}(r)$. The energy expectation value was computed in the FHNC/C approximation, using (as labeled) CW, JF, and PB expressions for the kinetic energy.

entering the wave function, as one might expect from the relatively low density of these systems. In fact, the magnitudes of the energy shifts produced by going from one choice of f to another are less than our best estimates of the numerical uncertainty (~ 0.1 K) in the evaluation of the energy expectation values. This estimate is arrived at by varying the grid sizes for the tabulated functions and numerical transforms involved in solution of the FHNC equations.

In Figs. 1–3 we have plotted the zero-temperature

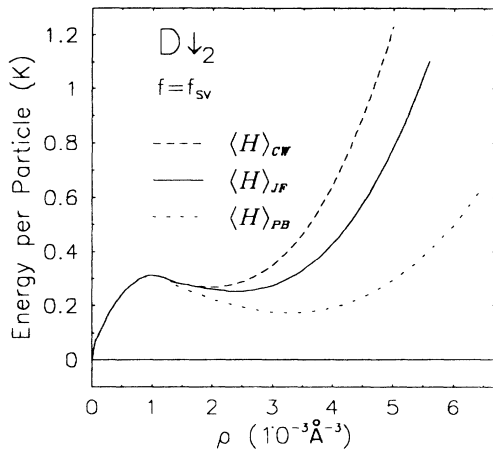


FIG. 2. Jastrow energy per particle versus density for the electron-spin-aligned deuterium system $D\downarrow_2$, based on the Kolos-Wolniewicz potential and the Schiff-Verlet correlation function $f_{SV}(r)$. The energy expectation value was computed in the FHNC/C approximation, using (as labeled) CW, JF, and PB expressions for the kinetic energy.

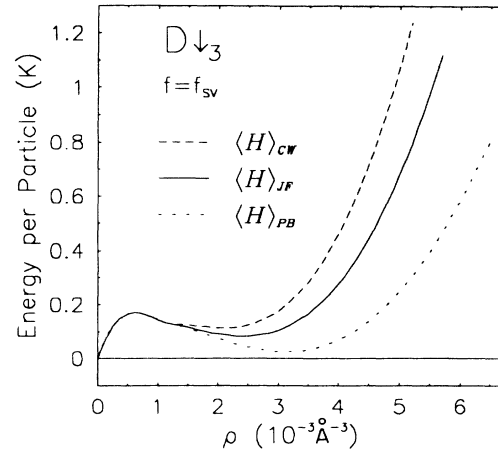


FIG. 3. Jastrow energy per particle versus density for the electron-spin-aligned deuterium system $D\downarrow_3$, based on the Kolos-Wolniewicz potential and the Schiff-Verlet correlation function $f_{SV}(r)$. The energy expectation value was computed in the FHNC/C approximation, using (as labeled) CW, JF, and PB expressions for the kinetic energy.

equations of state for the three species of $D\downarrow$, with the SV choice of f . The following qualitative comments apply to all three cases.

At small values of the density ρ , the FHNC/C approximations to $\langle H \rangle_{CW}$, $\langle H \rangle_{JF}$, and $\langle H \rangle_{PB}$ are nearly identical, since at low density the energy is dominated by the Fermi-gas component $T_F = 0.3\hbar^2 k_F^2 / 2m$. As ρ increases, the three expectation values begin to disagree. The discrepancies reflect the different ways in which the alternative forms of the kinetic energy express three-body correlation kinetic energy effects or effects due to the coupling between derivatives of the correlation operator and of the Slater determinant. In general, the CW prescription underestimates the binding energy; the PB expression overestimates the binding (indeed, $\langle H \rangle_{PB}$ does not even saturate for $D\downarrow_1$, as shown in Fig. 1); and the Jackson-Feenberg choice lies in between. Over most of the range of densities, $\langle H \rangle_{JF}$ is seen to be roughly the average of $\langle H \rangle_{CW}$ and $\langle H \rangle_{PB}$, approximating a relationship which is exact for Bose systems.

The disagreement among the different evaluations of $\langle H \rangle$, which becomes very prominent at higher densities, may be ascribed to the omission of elementary cluster diagrams,^{3,4} which become more and more important as the average particle separation decreases, and affect the three kinetic-energy formulas in different degrees. We should stress, however, that the size of the disparities is exaggerated by the energy scale used in the figures. While these disparities amount to only small percentages of either the potential energy $\langle V \rangle$ or the kinetic energy $\langle T \rangle$, they are large when compared to the total energy, which results from a near cancellation of $\langle T \rangle$ and $\langle V \rangle$. The absolute discrepancies in the deuterium systems are, in fact, much smaller than those found in studies of ^3He ; moreover, the spread between $\langle H \rangle_{CW}$ and $\langle H \rangle_{PB}$ grows less rapidly as the density is increased. It is therefore suggest-

ed that the elementary diagrams are less important for deuterium than for helium.

Energy curves $\langle H \rangle_{\text{JF}}$ for $D\downarrow_1$, $D\downarrow_2$, and $D\downarrow_3$ based on f_{opt} are displayed in Fig. 4. The locations of the finite-density minima of these Jastrow energies are roughly $3.7 \times 10^{-3} \text{ \AA}^{-3}$ ($\rho\sigma^3=0.185$) for $D\downarrow_1$ and $2.8 \times 10^{-3} \text{ \AA}^{-3}$ ($\rho\sigma^3=0.140$) for $D\downarrow_{2,3}$. (As convenient, we shall measure the density ρ in units of \AA^{-3} or by the dimensionless combination $\rho\sigma^3$, where $\sigma=3.6892 \text{ \AA}$ is the "zero-crossing" of a Lennard-Jones fit to the interatomic potential. The latter measure permits an easier comparison with other strongly-interacting quantum systems, notably ^3He .)

At this point we call attention to a striking qualitative feature of the available variational results for all three choices of f : namely, beginning at a relatively low density, the energy curve for $D\downarrow_1$ lies *below* the other two curves. This is contrary to the prediction of simple physical arguments,¹ which would lead one to believe that, at least for a state-independent potential and at not-too-high densities, the system with the largest level degeneracy should have the lowest-lying ground state.

Over most of the density range covered by Fig. 4, the results for $D\downarrow_2$ and $D\downarrow_3$ show a more reasonable behavior with respect to one another, in that $\langle H \rangle_{\nu=3}$ lies below $\langle H \rangle_{\nu=2}$ at given ρ . Nevertheless, at high density, the $D\downarrow_2$ curve does indeed drop below the curve for $D\downarrow_3$. Qualitatively, the differences between the equation-of-state results for $D\downarrow_2$ and $D\downarrow_3$ are not as prominent as between the results for either $D\downarrow_2$ or $D\downarrow_3$ and $D\downarrow_1$. This is in line with the observation that the parameter ν enters the FHNC/C calculations essentially as ν^{-1} , which makes a smaller "jump" as ν changes from 3 to 2 as compared to the change from 3 or 2 to 1.

The apparent energetic preference, within the Jastrow

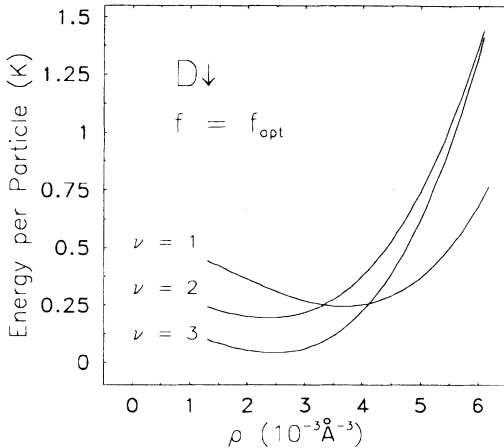


FIG. 4. Jastrow energy per particle versus density for three species of electron-spin-aligned deuterium $D\downarrow$, with (as labeled) one, two, or three equally populated nuclear spin states, based on the Kolos-Wolniewicz potential and the optimal correlation function $f_{\text{opt}}(r)$. The latter correlation function, as well as the energy expectation value, were determined within the FHNC/C approximation, using the Jackson-Feenberg (JF) expression for the kinetic energy.

description, for the fully-polarized system $D\downarrow_1$ over $D\downarrow_{2,3}$ parallels findings of detailed variational studies of ^3He .^{2,16,17} The conclusion in the case of liquid helium is that the Jastrow wave function does not give nearly so poor a description of the correlation structure for fully-polarized helium as it does for spin-saturated (ordinary) ^3He . Optimized triplet and backflow correlations, if included in the trial wave function, significantly lower the variational energy of the unpolarized phase, while having little effect on the nuclear-spin-polarized phase. Indeed, the expected ordering of the ^3He equations of state in the liquid-density range is recovered with the better variational wave function^{16,17} (see also Ref. 18).

Our system $D\downarrow_1$ can be considered the deuterium counterpart of nuclear-spin-aligned ^3He , since the deuteron spins, as well as the spins of the orbiting electrons, are considered to be fully polarized. Similarly, $D\downarrow_1$ is analogous to the normal phase of ^3He , and the higher-degeneracy species $D\downarrow_3$ should also resemble normal ^3He , for the purpose of qualitative comparisons between spin-saturated and fully-polarized systems. However, the apparent spin instability within the Jastrow description has a much weaker "signal" in $D\downarrow$ than in ^3He . Referring again to Fig. 4, two salient observations can be made. First, the level crossings in $D\downarrow_\nu$ are at densities greater than the equilibrium ($dE/d\rho=0$) densities for the three systems. This is in sharp contrast with the inversion at low density seen for the Jastrow equations of state in ^3He .² Second, the minimum energies for the three deuterium species at their equilibrium densities *are* consistent with the intuitive expectations mentioned above: the (finite-density) minimum of $\langle H \rangle$ versus ρ for $\nu=3$ lies below that for $\nu=2$, which in turn lies below the minimum for $\nu=1$.

Based on the FHNC/C results alone, the question of the ground-state phase of $D\downarrow$ would remain unresolved. If we adopt $\langle H \rangle_{\text{JF}}$ as the form of the energy expectation value most likely to provide a close upper bound, the minimum energy per particle for all three species is very small but positive. The true ground-state energy for any or all three of the systems could still be negative, and implying the existence of self-bound liquids.

The magnitude of $\langle H \rangle$ itself is less than the numerical uncertainty of the FHNC calculations. While the size of the differences between the three choices for the expectation value (viz., CW, JF, and PB) gives some idea of the magnitude of the errors associated with the approximations introduced in computing g and g_3 and hence $\langle H \rangle$, we have to go outside the FHNC scheme altogether to assess the absolute accuracy of the FHNC evaluation of the energy. Variational Monte Carlo evaluation of $\langle H \rangle$ provides such a check, and allows us to determine the zero-temperature equations of state with much greater confidence.

B. Monte Carlo results

The Jastrow wave function Ψ_J of (2.1) and (2.2) defines a probability density $P(R)=P_J(R)$ for configuration R . Following Ceperley *et al.*,¹⁹ the standard Metropolis Monte Carlo algorithm²⁰ is used to sample this $P(R)$, for the various deuterium cases, by a random walk in

configuration space and thereby to calculate the expectation value of the energy, assuming a finite number N of atoms at the given density in a finite box. As usual, the simulation box is replicated throughout all space to form a periodic lattice. For further relevant details, see Appendixes A and B.

Since it is the system most likely to be self-bound, we first look at $D\downarrow_3$. Some results for the ground-state energy of this system are displayed in Fig. 5 and Table I (cf. Ref. 5). For comparison, we have also included in Fig. 5 a corresponding curve for $\langle H \rangle_{\text{JF}}$ from Fig. 4. Paying close attention to the very fine energy scale used in Fig. 5, the finite-density minimum of the Monte Carlo $\langle H \rangle$ versus ρ curve is unequivocally negative in the case of optimal pair correlations, lying more than 4 standard errors from the zero-energy line. Given this negative variational upper bound, it was concluded in Ref. 5 that, even at the Jastrow level, $D\downarrow_3$ has a liquid ground state. This conclusion is contingent, of course, on the unimportance of finite-size corrections to the MC simulation, which has been confirmed by test calculations at larger N (viz., $N=99$ particles instead of $N=57$).

Over the density range involved, the Monte Carlo curve for $u = u_{\text{opt}}$ lies somewhat below its FHNC/C counterpart (evaluated from the JF energy expression). We do not, however, see any emphatic increase of the discrepancy with density, corresponding to the increasing importance of elementary-diagram effects absent from the FHNC/C treatment but present in the MC results. This feature may be traced to the fact that, for simplicity, the MC calculations of Table I and Fig. 5 were carried out assuming the same pair pseudopotential at *all* of the densities considered, namely the solution u_{opt} of the FHNC/C Euler equation at $\rho = 3.52 \times 10^{-3} \text{ \AA}^{-3}$. Use of optimal pair correlations appropriate to the lower and higher densities will bring down the Monte Carlo equation of state somewhat in those regions and especially at the high-density end.

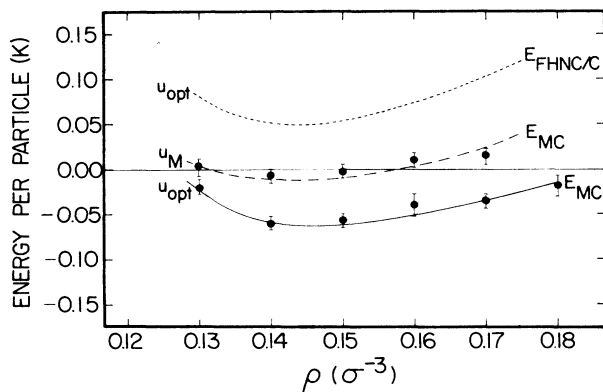


FIG. 5. Energy per particle versus density for $D\downarrow_3$ based on the Kolos-Wolniewicz potential. Solid curve: Jastrow energy for f_{opt} , computed by the Monte Carlo procedure. Short-dash curve: Jastrow energy for f_{opt} , calculated in the FHNC/C approximation. Long-dash curve: Jastrow energy for f_{SV} , with $b = 1.065\sigma$ (where $\sigma = 3.6982 \text{ \AA}$), computed by the Monte Carlo procedure. Optimal correlations f_{opt} were determined as for Fig. 4. The Monte Carlo results correspond to $N=57$ particles.

A comparison of the SV entries in Table I is more revealing, since for these the same density-dependent correlation function (with b optimized at *each density point*) was employed in both FHNC/C and MC calculations. Certain deficiencies of the FHNC/C approximation to the radial distribution function $g(r)$ now become apparent. True enough, we see that the FHNC/C values of the kinetic energy $\langle T \rangle$ agree rather well with the Monte Carlo values, especially at lower densities. With growing density, the gap between the FHNC/C and MC values for $\langle T \rangle$ widens somewhat, but this gap remains less than the sum of the numerical uncertainty of the FHNC/C procedure and the statistical uncertainty of the MC results. However, a much less satisfactory picture emerges for the potential energy.

The average potential energy per particle $\langle V \rangle$ is computed in both methods via

$$\langle V \rangle = \frac{\rho}{2} \int V(r)g(r)d^3r, \quad (2.7)$$

and is evidently more sensitive than $\langle T \rangle$ to errors in $g(r)$. At the lowest density listed, the difference between the FHNC/C and MC results for $\langle V \rangle$ alone accounts for the discrepancy in the total energy $\langle H \rangle$. With increasing density, the differences between the two evaluations of $g(r)$, and hence $\langle V \rangle$, become more pronounced, indicating that the elementary diagrams, simulated only very crudely in the solution of the FHNC/C equations, are important to an accurate $g(r)$, especially at densities around and above the equilibrium density. The corresponding omission of elementary-diagram effects leads to an *underestimate* of the magnitude of $\langle V \rangle$ at all densities examined.

Still concentrating on the SV results of Table I, we see that the FHNC/C procedure, with the Jackson-Feenberg form for the kinetic energy operator, yields an *overestimate* of $\langle T \rangle$. Combining this overestimated $\langle T \rangle$ with the FHNC/C underestimate for $\langle V \rangle$, the full energy expectation value $\langle H \rangle_{\text{JF}}$ may be regarded as a secure upper bound to the exact Jastrow energy.

Figure 6, which compares results of FHNC/C and MC energy-minimization searches for the optimal parameter b entering f_{SV} , provides additional information on the accuracy of the FHNC/C evaluation of $\langle H \rangle$. The relative shallowness of the upper curve attests to the fact that the FHNC/C Jastrow energy is much less sensitive to changes in b than is the MC energy. Even so, this comparison demonstrates one aspect of the computational efficiency of the FHNC/C scheme at the Jastrow level: although the absolute magnitude of the energy is in error, the value of b which minimizes $\langle H \rangle_{\text{JF}}$ in the FHNC/C approximation comes close to minimizing the energy in the more expensive Monte Carlo procedure. [We warn that this property cannot be attributed indiscriminately to FHNC evaluation in all contexts: for example, minimization of the FHNC/0 approximation in a σ_z -dependent variational treatment of ${}^3\text{He}$ leads to the wrong region of parameter space, judged in terms of the results of an accurate minimization within MC (see Ref. 21).]

Our Monte Carlo results for the Jastrow energy of $D\downarrow_1$ and $D\downarrow_2$ in the f_{SV} case are collected in Table II. To en-

TABLE I. Comparison of Fermi-hypernetted chain (FHNC) and Monte Carlo (MC) evaluations of Jastrow kinetic, potential, total energies (respectively, $\langle T \rangle$, $\langle V \rangle$, and $\langle H \rangle$), for $D\downarrow_3$. FHNC results correspond to the Jackson-Feenberg expression for the kinetic energy. All energies are in K per particle. Statistical errors in last decimal place of MC results are given in parentheses.

$(10^{-3} \text{ \AA}^{-3})$	$\rho\sigma^3$	Method	$\langle T \rangle$	f_{SV}^f $\langle V \rangle$	$\langle H \rangle$	$\langle T \rangle$	f_{opt}^f $\langle V \rangle$	$\langle H \rangle$
2.82	0.142	FHNC	3.43	-3.34	0.09	3.52	-3.47	0.05
		MC	3.42(2)	-3.43(1)	-0.01(1)	3.47(2)	-3.51(2)	-0.04(1)
3.52	0.177	FHNC	4.51	-4.34	0.17	4.59	-4.47	0.12
		MC	4.45(3)	-4.43(2)	0.02(1)	4.45(3)	-4.50(2)	-0.05(1)
4.23	0.213	FHNC	5.71	-5.36	0.35	5.76	-5.46	0.30
		MC	5.62(3)	-5.48(2)	0.14(2)	5.54(4)	-5.46(3)	0.08(2)
4.93	0.248	FHNC	7.05	-6.42	0.63	7.05	-6.48	0.57
		MC	6.96(5)	-6.64(3)	0.32(2)	6.73(4)	-6.39(3)	0.34(3)
5.63	0.283	FHNC	8.50	-7.43	1.07	8.57	-7.54	1.03
		MC	8.44(7)	-7.71(4)	0.73(4)	8.10(4)	-7.40(4)	0.70(3)
6.34	0.318	FHNC	10.13	-8.44	1.69	10.14	-8.49	1.65
		MC	9.91(7)	-8.78(5)	1.13(5)	9.40(5)	-8.30(5)	1.10(3)

sure clean comparisons, as with $D\downarrow_3$, the same values for the ρ -dependent variational parameter b which minimized $\langle H \rangle_{JF}$ in the FHNC/C treatment were used in the Monte Carlo calculations. Looking at $D\downarrow_2$, the Jackson-Feenberg FHNC/C results consistently lie above the MC results. At high density, $\langle T \rangle_{FHNC/C}$ does not overestimate the exact kinetic energy, but the substantial underestimate of $\langle V \rangle$ is more than sufficient to keep the FHNC/C evaluation of $\langle H \rangle_{JF}$ an upper bound to the accurate MC $\langle H \rangle$.

The results for $D\downarrow_1$ exemplify the misleading nature of canceling errors. While the FHNC/C evaluation of the full energy expectation value $\langle H \rangle_{JF}$ agrees well with the MC result, the agreement is due to the combined effects of underestimation of both $\langle T \rangle_{FHNC/C}$ and $|\langle V \rangle_{FHNC/C}|$. At intermediate densities, the FHNC/C energy even falls below the MC energy.

Comparing the $\langle V \rangle_{MC}$ entries from Tables I and II, we see that the potential energy components for the three

species of $D\downarrow$ are virtually the same, so the differences between their Jastrow energies come almost exclusively from the kinetic energy.

We also performed Monte Carlo calculations on $D\downarrow_1$ and $D\downarrow_2$ using f_{opt} , with results similar to those obtained for f_{SV} . To wit: the MC values for $\langle H \rangle$ are lower than the FHNC/C values for $\langle H \rangle_{JF}$ by about 0.1 K near the finite density minimum in the case of $D\downarrow_2$, while the JF-FHNC/C and MC values for $\langle H \rangle$ in $D\downarrow_1$ are, again, very close, even though the respective evaluations $\langle T \rangle$ and $\langle V \rangle$ differ considerably. For neither $D\downarrow_1$ nor $D\downarrow_2$ does the Monte Carlo energy-versus-density curve based on f_{opt} go negative. At the two-body Jastrow level, then, while $D\downarrow_3$ is clearly a self-bound liquid, we are still confronted with very small but positive upper bounds on the ground-state energies of $D\downarrow_1$ and $D\downarrow_2$, leaving the nature of their respective ground-state phases in doubt.

Before we turn to MC calculations for non-Jastrow correlations and compare their results with those from CBF perturbation theory, a brief digression on the errors associated with the variational Monte Carlo method is in order. The most obvious errors are statistical in nature; to deal with these, the calculations may simply be "run longer" or variance reduction techniques employed. In addition, there might be significant finite-size effects, in which case the results of the Monte Carlo calculation may not faithfully represent the properties of the infinitely extended, bulk fluid. For the calculations reported in this paper, such finite-size effects introduce an uncertainty of less than 0.02 K in the energy over the density ranges studied. This estimate was arrived at by repeating the calculations at a fixed density for larger numbers of particles in a larger simulation box.

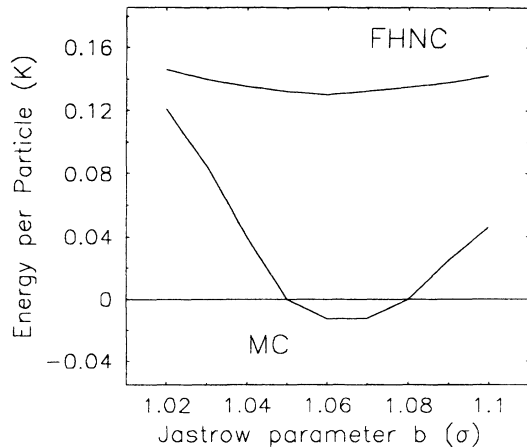


FIG. 6. Comparison of energy-minimization searches for optimal parameter b in Schiff-Verlet correlation function f_{SV} . Jastrow energies were calculated by (as labeled) FHNC/C and Monte Carlo (MC) methods.

III. BEYOND THE JASTROW MODEL

We now improve upon the Jastrow description given by Eqs. (2.1) and (2.2), with the primary aim of determining the nature of the ground-state phases of $D\downarrow_1$ and $D\downarrow_2$. The correlation operator F appearing in (2.1) is general-

TABLE II. Comparison of Fermi-hypernetted chain (FHNC) and Monte Carlo (MC) evaluations of Jastrow kinetic, potential, and total energies (respectively, $\langle T \rangle$, $\langle V \rangle$, and $\langle H \rangle$), for $D\downarrow_1$ and $D\downarrow_2$, assuming Schiff-Verlet correlations. FHNC results correspond to the Jackson-Feenberg expression for the kinetic energy. All energies are in K per particle. Statistical errors in last decimal place of MC results are given in parentheses.

$(10^{-3} \text{ \AA}^{-3})$	$\rho\sigma^3$	Method	$\langle T \rangle$	$D\downarrow_1$ $\langle V \rangle$	$\langle H \rangle$	$\langle T \rangle$	$D\downarrow_2$ $\langle V \rangle$	$\langle H \rangle$
2.82	0.142	FHNC	3.39	-3.06	0.33	3.49	-3.23	0.26
		MC	3.57(3)	-3.23(1)	0.34(1)	3.47(2)	-3.32(2)	0.15(1)
3.52	0.177	FHNC	4.40	-4.10	0.30	4.55	-4.22	0.33
		MC	4.55(3)	-4.25(2)	0.30(1)	4.53(3)	-4.33(2)	0.20(1)
4.23	0.213	FHNC	5.36	-5.06	0.30	5.72	-5.24	0.48
		MC	5.75(3)	-5.43(2)	0.32(2)	5.69(4)	-5.42(2)	0.26(2)
4.93	0.248	FHNC	6.50	-6.11	0.39	6.99	-6.24	0.75
		MC	6.96(3)	-6.48(3)	0.48(2)	7.02(4)	-6.51(3)	0.51(2)
5.63	0.283	FHNC	7.63	-7.07	0.56	8.35	-7.23	1.12
		MC	8.28(4)	-7.64(4)	0.64(2)	8.43(4)	-7.57(4)	0.86(2)
6.34	0.318	FHNC	8.79	-8.04	0.75	9.85	-8.22	1.63
		MC	9.83(6)	-8.77(4)	1.06(3)	10.07(5)	-8.70(5)	1.37(3)

ized to include triplet and backflow correlations as well as the state-independent pair correlations of the product $F_J = \prod_{i < j} f(r_{ij})$.

Some useful information about non-Jastrow correlations is available from a recent study⁶ of the deuterium systems $D\downarrow_2$ and $D\downarrow_3$ within the method of correlated basis functions (CBF). In an analysis of the energy closely paralleling that carried out for ^3He by Krotscheck and Smith,²² the second- and third-order CBF corrections in a Jastrow-correlated basis were examined, the relevant CBF matrix elements being determined by FHNC/C-FHNC/C' techniques, to the level of factorizable diagrams.^{2,23} The correlated $2p$ - $2h$ and $3p$ - $3h$ contributions to the second correction (denoted, respectively, $\delta E_2^{(2)}$ and $\delta E_3^{(2)}$), as well as the correlated $2p$ - $2h$ contribution $\delta E_2^{(3)}$ to the third-order correction, have been numerically evaluated. The latter contribution is made up of particle-particle, hole-hole, and ring terms. The calculated $2p$ - $2h$ correction terms introduce the leading effects of (spin-) density fluctuations and propagator corrections, while the $3p$ - $3h$ term incorporates the leading effect of triplet correlations. The $\nu=1$ system was not treated because of a spurious instability which is well understood (cf. Ref. 24) but necessitates rearrangement of the CBF perturbation series.

The following findings of this CBF study provide valuable clues to the construction of an improved ground-state trial function.

(a) In both $D\downarrow_2$ and $D\downarrow_3$, the $2p$ - $2h$ second-order correction $\delta E_2^{(2)}$ is sizable compared to H_{00} , indicating that state- and energy-dependent effects absent from the Jastrow description are important for both systems, if one seeks to determine the energy to the 0.1-K level of accuracy or below. Among other things, this term contains the leading energetic manifestation of "backflow."

(b) The third-order pp and hh contributions are quite small for both systems. We take this to mean that the short-range two-body correlations induced by the nearly

hard core of the bare interaction are adequately handled by the Jastrow wave function. Only the ring term shows the potential of interfering with a rapid convergence of the $2p$ - $2h$ subseries of the CBF perturbation expansion.

(c) The second-order $3p$ - $3h$ correction is small for densities below equilibrium in both systems, but at densities near and above equilibrium, this term becomes substantial, implying that three-body correlations are important at higher densities.

Triplet factors and momentum-dependent correlations may be directly incorporated into the correlated basis functions, with consequent reduction in the size of CBF corrections. However, this generalization greatly complicates the task of diagrammatic evaluation of the relevant CBF matrix elements (cf. Ref. 16), necessitating further approximations and thereby significantly increasing the numerical uncertainty in the resulting energies. By contrast, upon *suitable* generalization^{25,26} of the ground-state trial function to include triplet correlations and backflow (*as described below*), variational Monte Carlo evaluation of the energy expectation value proceeds in a straightforward (albeit computationally more intensive) manner, without the need for any significant revision of the MC routine applied in the Jastrow case.

Explicit three-body (or triplet) correlations may be incorporated into the correlation operator F of (2.1) by generalizing upon the pseudopotential $u = -2 \ln f$ appearing in the Jastrow ansatz. More specifically, $F_J(R)$ is replaced by^{25,26}

$$F_{2,3}(R) = \exp \left[-\frac{1}{2} \sum_{i < j} \hat{u}(r_{ij}) - \frac{\lambda_T}{4} \sum_{i < j} \sum_l \xi(r_{li}) \xi(r_{lj}) \mathbf{r}_{li} \cdot \mathbf{r}_{lj} \right], \quad (3.1a)$$

wherein

$$\hat{u}(r) = u(r) - \lambda_T \xi^2(r) r^2. \quad (3.1b)$$

While $F_{2,3}^2$ retains the form $\exp[-\sum_{i<j} \bar{u}(ij)]$, the pseudopotential $\bar{u}(ij)$ now contains a noncentral component involving a third particle. We may choose the central quantity $u(r)$ essentially as before, in correspondence with Schiff-Verlet, Pandharipande-Bethe, and optimal choices of the two-body Jastrow correlation function $f(r)$. However, the introduction of three-body correlations will generally necessitate some reoptimization of the genuine two-body correlations. There remains the question of how the function $\xi(r)$ is to be chosen. In their study of the ground state of ^3He , Levesque and Lhuillier²⁷ employed the form

$$\xi(r) = \frac{m}{2} \frac{b^m}{r^{m+2}} e^{-(1/r)^m}, \quad (3.2)$$

where the parameters b and m were taken the same as in the form $u(r) = (b/r)^m$ which these authors adopted for the original two-body pseudopotential. The correlations induced by (3.2) are of medium range, and this choice favors equilateral configurations of a triplet. A second form for ξ was used by Schmidt *et al.*^{25,26} in their simulations of ^3He and ^4He , namely

$$\xi(r) = \exp \left[- \left[\frac{r - r_T}{w_T} \right]^2 \right], \quad (3.3)$$

where r_T and w_T fix the center and the width of the Gaussian, respectively. Along with λ_T , the latter quantities become new variational parameters in the energy minimization. The corresponding choice of triplet correlations is again effective at medium ranges, say, interparticle spacings of σ to 2σ . We have adopted the form (3.3) in our calculations on $\text{D}\downarrow$.

Momentum-dependent correlations may be built into the trial wave function by a simple alteration upon the orbitals which make up the Slater determinant. The replacement

$$\det[\exp(i\mathbf{k}_i \cdot \mathbf{r}_j)] \rightarrow \det \left\{ \exp \left[i\mathbf{k}_i \cdot \left(\mathbf{r}_j + \sum_{l \neq j} \eta(r_{lj}) \mathbf{r}_{lj} \right) \right] \right\} \quad (3.4)$$

generates backflow effects in the spirit of Feynman and Cohen,²⁸ a fact already exploited in Monte Carlo studies of ^3He (Refs. 25 and 26). Following that earlier work, the function $\eta(r)$ is here taken to have the form

$$\eta(r) = \lambda_B \exp \left[- \left[\frac{r - r_B}{w_B} \right]^2 \right] + \frac{\lambda'_B}{r^3}, \quad (3.5)$$

where λ_B , λ'_B , r_B , and w_B are new variational parameters referring specifically to the backflow correlations.

Unless precautions are taken, the required periodic boundary conditions are destroyed if the range of the correlations extends beyond the walls of the simulation cube. Since the elemental box contains a fixed number of particles, detrimental effects would be most noticeable at high densities where the box size is smaller. For the most part, the correlations present in the deuterium systems are of quite short range, so this is not a serious problem. Nevertheless, we obviate potential errors from this source by

using *reflected* correlations (of, respectively, central, triplet, and backflow character) where appropriate, i.e.,

$$f(r) \rightarrow f(r) + f(2r_{\max} - r) - 2f(r_{\max}). \quad (3.6)$$

Owing to the short-range nature of the original correlations, this finite-size adaptation has no appreciable energetic effect; it serves only to guarantee that the correlations go smoothly to zero at r_{\max} , i.e., at the sides of the simulation cube.

The probability distribution sampled in the Monte Carlo procedure now corresponds to the trial function elaborated as above. The essential numerical consequences are the following.

Triplet correlations given by Eqs. (3.1) and (3.3), with optimally determined parameters $\lambda_T = -1.2$, $r_T = 0.66\sigma$, and $w_T = 0.50\sigma$, lower the energy per particle in $\text{D}\downarrow_3$ by about 0.1 K over the range of densities studied. Backflow correlations, described by (3.4) and (3.5), with optimal parameters $\lambda_B = 0.14$, $r_B = 0.74\sigma$, $w_B = 0.54\sigma$, and $\lambda'_B = 0.15$, yield a further reduction of roughly 0.1 K. These findings strengthen our earlier conclusion, within the Jastrow framework, that the ground-state phase of $\text{D}\downarrow_3$ is a self-bound liquid.

Turning to $\text{D}\downarrow_2$, a calculation was performed with the triplet and backflow parameters determined for $\text{D}\downarrow_3$. While this does not result in a large energy gain, the downward shift from the Jastrow $\langle H \rangle$ is nevertheless sufficient to bring the equation of state for $\text{D}\downarrow_2$ below the zero-energy axis. We conclude, therefore, that $\text{D}\downarrow_2$ is also a self-bound liquid.

The refined Monte Carlo equations of state are displayed in Fig. 7. An improved equation of state for $\text{D}\downarrow_1$ (based also on the parameters found to be optimal for $\text{D}\downarrow_3$) is given as well. In fact, triplet and backflow correlations in $\text{D}\downarrow_1$, introduced in this manner, have negligible effect. This finding supports our contention that the Jastrow wave function aptly represents the ground state of the fully polarized system. The data corresponding to the MC curves of Fig. 7 are listed in Table III.

For comparison, Fig. 7 also includes equations of state for $\text{D}\downarrow_2$ and $\text{D}\downarrow_3$ derived from CBF perturbation theory. These curves were constructed by adding the available second- and third-order CBF corrections (taken from Tables I and II of Ref. 2, which are based on f_{opt}) to the *Monte Carlo* Jastrow energies for f_{opt} . The latter represent, of course, an accurate evaluation of the leading ("variational") term in the exact Jastrow-CBF perturbation expansion. Unlike the perturbation corrections, which are evaluated using the FHNC/C approximation for the CBF matrix elements, this leading (and dominant) term does not suffer from errors due to inadequate treatment of elementary diagrams.

Qualitatively, the predictions of these CBF and refined MC descriptions of $\text{D}\downarrow_2$ and $\text{D}\downarrow_3$ are in accord: both species of spin-aligned deuterium would be self-bound liquids in their ground states, with $\text{D}\downarrow_3$ energetically lower than $\text{D}\downarrow_2$ over the whole liquid-density range. Further, the energy of $\text{D}\downarrow_1$ lies above the energies for $\text{D}\downarrow_2$ and $\text{D}\downarrow_3$ at all densities considered, resulting in the expected ordering in the relative stabilities of the three phases. Three

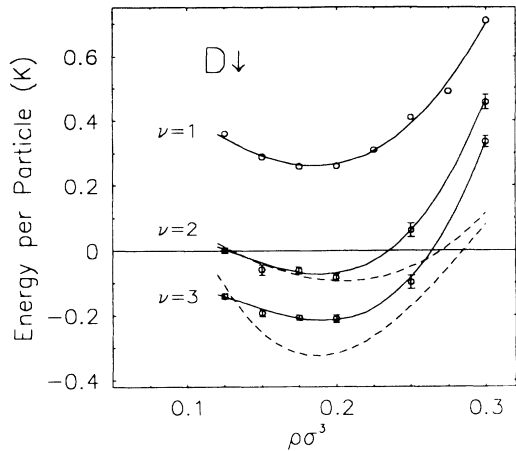


FIG. 7. Energy per particle versus density for three species of electron-spin-aligned deuterium $D\downarrow$, with (as labeled) one, two, or three equally populated nuclear spin states, based on the Kolos-Wolniewicz potential. Solid curves: Equations of state for improved variational wave function including optimal Jastrow, triplet, and backflow correlations, calculated by the Metropolis Monte Carlo method. Dashed curves: CBF equations of state, formed by adding the Monte Carlo-computed Jastrow energy for f_{opt} , taken from Fig. 4, and the available FHNC/C results for the leading CBF corrections.

cautionary remarks are in order here. The first is that although the convergence of the CBF perturbation expansion looks reasonably good in the relevant density range, the size of the highest-order terms which have been evaluated is not sufficiently small that a firm conclusion can be reached about the ground-state phase of $D\downarrow_2$ on the basis of the CBF results alone. The second point is that if we extrapolate the CBF curves into the high-density region, the estimated energy of $D\downarrow_2$ drops below that of $D\downarrow_3$ at about twice equilibrium density. And finally, we must reiterate that no CBF corrections have yet been calculated for $D\downarrow_1$; with their inclusion the corresponding curve in Fig. 7 would come down, but presumably not very far.

Quantitatively, at densities near and below equilibrium density, the MC and CBF curves for $D\downarrow_2$ show remarkable agreement. At higher densities, the CBF energies are somewhat lower than the MC values. In the case of $D\downarrow_3$,

TABLE III. Energy per particle vs density for three species of electron-spin-aligned deuterium $D\downarrow$, evaluated by the variational Monte Carlo procedure, for improved wave function including optimal Jastrow, triplet, and backflow correlations. Statistical errors in the last decimal place are given in parentheses.

$\rho\sigma^3$	$D\downarrow_1$	$D\downarrow_2$	$D\downarrow_3$
0.125	0.36(1)	0.00(1)	-0.14(1)
0.150	0.29(1)	-0.06(1)	-0.19(1)
0.175	0.26(1)	-0.06(1)	-0.21(1)
0.200	0.26(1)	-0.08(1)	-0.21(1)
0.250	0.41(2)	0.06(2)	-0.10(2)
0.300	0.71(2)	0.46(2)	0.34(2)

the CBF equation of state lies below the MC energy curve, the difference between the two curves remaining constant over most of the liquid-density regime.

The reasons for the differences (or the agreement) between the CBF and MC curves for $D\downarrow_2$ and $D\downarrow_3$ is not easy to determine in detail. The Monte Carlo curves are accurate equations of state for the given finite number of deuterium atoms in a periodically replicated box, described by a trial wave function having two-body Jastrow, triplet, and backflow correlations, for the given set of parameters. A more extensive search in parameter space, or the adoption of other functional forms for the correlations, could alter the MC equations of state, although we believe any such changes would be small. On the other hand, we have no reliable measure of the accuracy of the truncated CBF perturbation expansion. There is, however, the general expectation that the second-order CBF perturbation correction will overestimate the energy lowering due to correlations beyond the Jastrow model, and the expectation, in the present context, that the errors in the CBF description are not large.

One noteworthy difference between the CBF and MC evaluations, evident in Fig. 7, is in their results for the finite-density energy minima. The Monte Carlo curves for all three species of spin-aligned deuterium yield the same equilibrium density, $\rho_0 = 4.0 \times 10^{-3} \text{ \AA}^{-3}$ ($\rho\sigma^3 = 0.20$). The CBF curves locate the minima at positions about 10% higher than this for $D\downarrow_2$ and about 10% lower for $D\downarrow_3$.

At this point we are unable to predict, with certainty, the zero-temperature phase of $D\downarrow_1$ from either Monte Carlo or correlated-basis-perturbation-theory calculations. The small but positive upper bound for the ground-state energy of this system may be depressed appreciably by some class of correlations not yet considered. However, initial results from advanced Green's function Monte Carlo calculations (cf. Refs. 29 and 30) indicate that any such lowering of the energy will be small.

From our microscopic study we conclude, then, that spin-aligned deuterium may well have a ground-state phase that depends on the scenario by which the atoms are produced, sorted, stabilized, concentrated, and confined: $D\downarrow$ would be a self-bound Fermi liquid if only the electron spins are aligned, as in $D\downarrow_3$ or $D\downarrow_2$. On the other hand, if this novel substance is purified in a form in which both nuclear and electronic spins are fully polarized, as in $D\downarrow_1$, it may remain in the gaseous state down to absolute zero, like the Bose system $H\downarrow$. The latter version of $D\downarrow$ might, in practice, be realized as "doubly polarized" deuterium, $D\downarrow\uparrow$, with the electronic and nuclear spins directed antiparallel to an imposed magnetic field (cf. Refs. 9–11). As an interesting consequence of the Fermi nature of this system, the extremely small ground-state energy at equilibrium (less than 0.25 K per particle) implies that at $T=0$ it would liquify under very slight, if not zero, pressure.

IV. OTHER GROUND-STATE PROPERTIES

Given a trial wave function determined variationally, the Monte Carlo procedure may, of course, be used to

evaluate the expectation values of other physical quantities besides the energy. Such expectation values generally do not possess the upper-bound property, and there is no guarantee that the physical quantities in question will be accurately predicted even if the trial wave function gives a close upper bound on the energy. However, we have seen that in the present problem the energy is a very small difference between relatively large kinetic and potential contributions; from all indications the individual kinetic and potential components are given rather accurately by the MC calculations recounted in Sec. II, and especially those described in Sec. III. This consideration justifies a serious examination of the radial distribution functions $g(r)$ corresponding to the trial functions we have generated [along with the associated static structure functions $S(k)$]. Likewise, it is of interest to evaluate, by Monte Carlo sampling, the one-body density matrix $n(r)$ [and associated momentum distribution $n(k)$] implied by these wave functions, although the kinetic energy was not actually computed directly in terms of this quantity. For some technical information on the Monte Carlo treatment of these additional properties of the system, see Appendix B. Here we shall focus on selected numerical results for the Jastrow trial functions.

Figure 8 gives plots of the two-body radial distribution functions $g(r)$ obtained from both FHNC/C and MC Jastrow calculations near the finite-density energy minima obtained for $D\downarrow_3$, based on the Schiff-Verlet correlation function. Figure 9 displays $g(r)$ results, also for $D\downarrow_3$ with f_{SV} , at a significantly higher density. In both cases it is seen that the FHNC/C curve has less structure than the MC curve, the difference being somewhat more pronounced at the higher density. This behavior is in accord with our results (discussed in Sec. II) for the average potential energy per particle $\langle V \rangle$: the neglect of the elementary-diagram effects by the FHNC/C approximation for $g(r)$ becomes more serious as the density increases.

Results for the static structure function corresponding

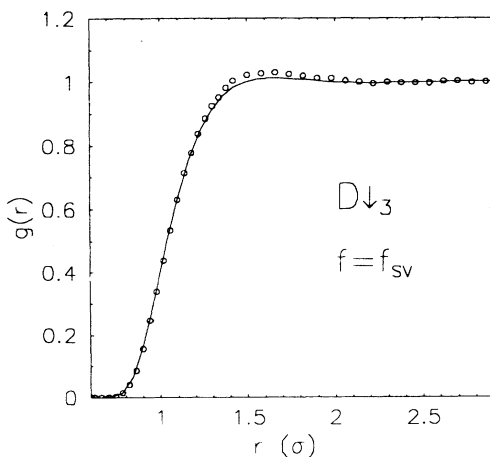


FIG. 8. Jastrow radial distribution function $g(r)$ for $D\downarrow_3$ at a density $\rho = 3.52 \times 10^{-3} \text{ \AA}^{-3}$. Solid curve: FHNC/C results. Circles: Monte Carlo results.

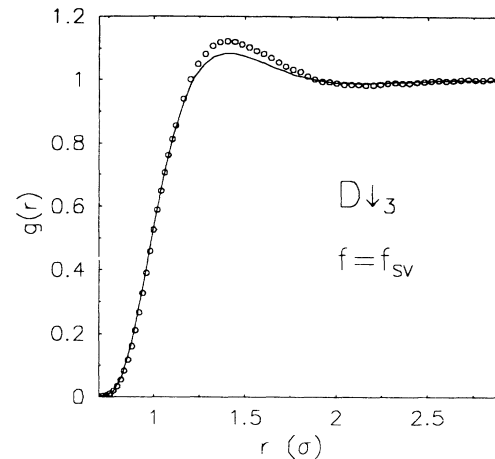


FIG. 9. Jastrow radial distribution function $g(r)$ for $D\downarrow_3$ at a density $\rho = 5.63 \times 10^{-3} \text{ \AA}^{-3}$. Solid curve: FHNC/C results. Circles: Monte Carlo results.

to the case considered in Fig. 8 is shown in Fig. 10. The low- k behavior of the FHNC/C version of $S(k)$ is correct by construction. The MC points plotted in the figure are obtained by transforming data for $g(r)$, although direct sampling of $S(k)$ would produce similar results for the discrete values of k in the simulation volume.

Figure 11 exhibits some results, near equilibrium, for the Jastrow one-body density matrix in the three species of $D\downarrow_1$, while Fig. 12 presents results for the Jastrow momentum distribution in $D\downarrow_3$ at a fairly low density. Again, FHNC/C and MC predictions are compared for the same Schiff-Verlet correlations. The FHNC curves for $n(r)$ and $n(k)$ were calculated by Flynn.³¹ Adopting a Jastrow approximation to the ground state of a strongly-interacting Fermi system, Ristig and Clark³² obtained general structural results for $n(k)$. With this work as a foundation, Fantoni³³ applied FHNC techniques to

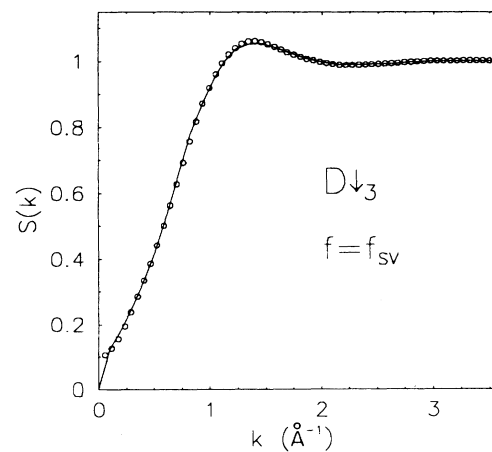


FIG. 10. Jastrow static structure function $S(k)$ for $D\downarrow_3$ at a density $\rho = 3.52 \times 10^{-3} \text{ \AA}^{-3}$. Solid curve: FHNC/C results. Circles: Monte Carlo results.

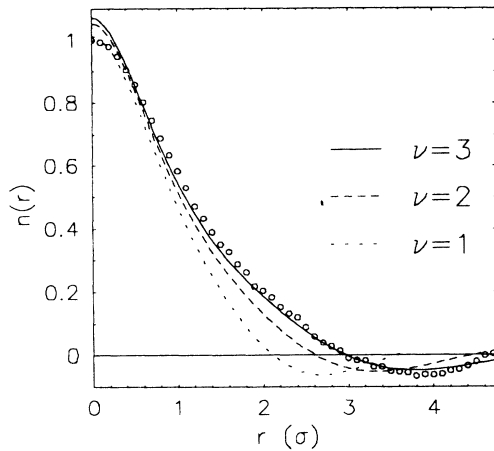


FIG. 11. Jastrow one-body density matrix $n(r)$ for three species of $D\downarrow_1$ at a density $\rho=3.52 \times 10^{-3} \text{ \AA}^{-3}$, based on f_{sv} . Curves represent results calculated in FHNC/0 approximation; circles are Monte Carlo data.

sum the irreducible cluster expansions determining the Jastrow $n(k)$. Flynn's results were obtained by solution of the integral equations which accomplish these summations at the FHNC/0 level of accuracy.

Further information on the momentum distribution in the spin-aligned deuterium systems may be found in Ref. 6. In particular, the available predictions for the quasiparticle pole strength z_{k_F} , as determined from the discontinuity of $n(k)$ at the Fermi surface, indicate that $D\downarrow_2$ is slightly less strongly correlated than is $D\downarrow_3$, and $D\downarrow_1$, in turn, is less strongly correlated than $D\downarrow_2$. In the $D\downarrow$ systems, z_{k_F} takes values intermediate between those of symmetrical nuclear matter and liquid ^3He at appropriately scaled densities: accordingly, electron-spin-aligned deuterium is a more strongly coupled Fermi fluid than nuclear matter, but is significantly less strongly coupled than ^3He .

ACKNOWLEDGMENTS

Much of this work was performed while R.M.P. was affiliated with the Courant Institute of Mathematical Sciences, New York University, where support was received from the Division of Materials Research of the U. S. National Science Foundation, under Grant No. DMR-8513300. This research was supported at Los Alamos National Laboratory by the U. S. Department of Energy and at Washington University by the Condensed Matter Theory Program of the Division of Materials Research of the U. S. National Science Foundation under Grant No. DMR-8519077.

APPENDIX A: VARIANCE REDUCTION TECHNIQUES

Metropolis Monte Carlo simulation has served as an almost indispensable tool in quantitative variational studies of equations of state of both classical and quantum systems. An important aspect of a reliable variational Monte

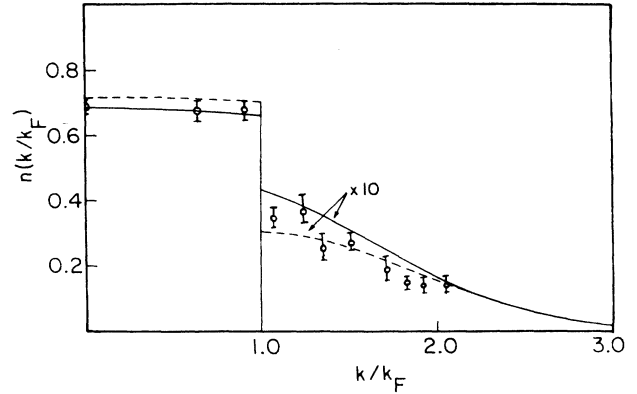


FIG. 12. Jastrow momentum distribution $n(k)$ of $D\downarrow_3$ at a density $\rho=2.98 \times 10^{-3} \text{ \AA}^{-3}$. Curves represent results calculated in FHNC/0 approximation. Solid curve: with f_{sv} . Dashed curve: with f_{opt} . Circles with error bars: Monte Carlo values for discrete values of k in simulation cube, based on f_{sv} .

Carlo quadrature, however, must be understood: in each step of the calculation, one must pay as much attention to the variance and standard error of the mean as to the mean itself. This is especially true in the present study, since our goal is to improve upon earlier calculations, which have demonstrated a remarkably close cancellation of positive and negative terms in the energy computation. Hence, we are confronted with a situation in which the energy expectation value is of small magnitude compared to its parts; but in order to address properly the question of the ground-state phase of our model system, the standard error associated with the energy expectation value must be reduced to a value much less than the energy itself.

The standard error in the Monte Carlo energy calculation declines as $m^{1/2}$, where m is the number of times the energy is sampled. In our calculation, m is of necessity very large, so care is taken to avoid the growth of numerical noise generated (for example) by roundoff or truncation. One such approach is to make several independent walks and to average the resulting energies. This approach injects into our computational task a flavor of experimental physics: one can expend effort in making a very precise measurement, or one can instead make many measurements which may not be very precise individually, but which have a precise mean value.

In FHNC theory, an important consideration in choosing the kinetic energy operator is the sensitivity of the corresponding energy expectation value to small errors in the radial distribution functions. In that case, the JF form has been found to be the most reliable, in that it is least sensitive to such errors, particularly errors in the sequential relation between the two- and three-particle spatial distribution functions.³⁴

On the other hand, in our application of the Monte Carlo scheme¹⁹ based on the Metropolis algorithm,²⁰ the three forms for the mean energy expectation value agree within statistics for an equilibrated system; that is, there is enough overlap of the three mean values broadened by

their respective error bars to make them statistically indistinguishable. The relevant figure of merit becomes the magnitude of the variance about the mean value as opposed to the mean value itself. Effort is focused, therefore, on reducing the variance sufficiently to be able to calculate the differences between the energy expectation values of the various choices for the trial ground-state wave function. In this regard, the variance of the PB form for the energy has proven to be smaller than for the JF form, and even more strongly preferred relative to the CW prescription. The PB form is therefore the superior choice. Naturally, a necessary but not sufficient condition that the Metropolis walk has reached its equilibrium distribution is the achievement of statistical agreement between the different energy estimators.

Because the Hamiltonian operator acts in a straightforward way on the trial function Ψ_T , the PB estimator is usually referred to in the Monte Carlo vocabulary as the "basic principles," or BP estimator. More precisely, within the Monte Carlo scheme we express the energy per particle, i.e., the expectation value per particle of the Hamiltonian H of the N -particle system, as the average

$$E = \langle H \rangle = N^{-1} \left\langle \frac{H\Psi_T}{\Psi_T} \right\rangle = \langle V_i + 2T_i - \mathbf{F}_i^2 \rangle, \quad (\text{A1})$$

where i refers to an arbitrary particle. Here T_i is a surrogate kinetic-energy operator,

$$T_i = -\frac{\hbar^2}{4m} \nabla_i^2 \ln \Psi_T, \quad (\text{A2})$$

and the potential energy operator is

$$V_i = \frac{1}{2} \sum_{i \neq j} \nu(ij), \quad (\text{A3})$$

where $\nu(ij)$ is the interatomic pair potential.

The "pseudoforce" \mathbf{F}_i appearing in the final form on the right of Eq. (A1) is defined by

$$\mathbf{F}_i^2 = \frac{\hbar^2}{2m} (\nabla_i \ln \Psi_T)^2. \quad (\text{A4})$$

Since the kinetic energy is identically equal to the mean-square pseudoforce,³⁵ we could choose a simpler estimator, for instance just the sum of the kinetic and potential energy estimators $\langle T_i \rangle$ and $\langle V_i \rangle$, but the near cancellation of these terms throughout the walk would lead to a very large variance. The variance of the estimator (A1) is much smaller, and the quality of the mean per unit computing effort is therefore much greater.

Another important variance reduction technique is the use of expected values, so that no information about rejected moves need be discarded. The simplest energy averaging scheme would be to add the energy at the new configuration if the move is accepted, and otherwise to add the energy of the old configuration. In averaging the *expected value* of an estimator, however, information about the rejected moves is also included. Hence, we can reduce the variance by averaging

$$E_{\text{exp}} = pE(R') + (1-p)E(R), \quad (\text{A5})$$

where p is the probability of accepting the move to R' from R , and $(1-p)$ is (obviously) the probability that the move is rejected. Every configuration, then, contributes to the energy in proportion to its likelihood of being realized. The same averaging procedure is also used for estimating other properties of the ground state.

APPENDIX B: MONTE CARLO EVALUATION OF DISTRIBUTION FUNCTIONS

A valuable product of variational Monte Carlo calculations is a representation of the trial wave function Ψ_T (or the associated probability density) in terms of an ensemble of configurations of particle positions. These configurations can be used to compute various properties of the system besides the energy, either during the course of the random walk, or by analyzing stored configurations of the system.

Of particular interest, both in itself and as an internal check on the consistency of the calculation, is the radial distribution function $g(\mathbf{r})$, which measures the probability of finding two particles separated by a distance r :

$$g(\mathbf{r}) = \frac{1}{N\rho} \sum_{i \neq j} \langle \delta(\mathbf{r}_i - \mathbf{r}_j - \mathbf{r}) \rangle. \quad (\text{B1})$$

(The angular brackets mean expectation value with respect to Ψ .) For an infinite, homogeneous, isotropic system, the function $g(\mathbf{r})$ depends only on the magnitude r of \mathbf{r} ; for asymptotically large r , $g(r)$ approaches unity. As each particle i is moved during a Monte Carlo run, the pair distances from the new and old positions of i to the other $N-1$ particles are recorded. Expected values are calculated in the same manner as for the energy: after the Metropolis acceptance ratio

$$p = \min[1, |\Psi_T(R_{\text{new}})/\Psi_T(R_{\text{old}})|] \quad (\text{B2})$$

has been determined, p is added to each bin recording $g(r)$ for each value of r_{ij} which is realized in the proposed configuration R_{new} , while $q = (1-p)$ is added to each $g(r)$ bin for the pair separations in the old configuration R_{old} .

The Fourier transform of $\rho[g(\mathbf{r})-1]$ yields $S(\mathbf{k})-1$, where $S(\mathbf{k})$ is the static structure function, which would be given directly by

$$S(\mathbf{k}) = N^{-1} \left\langle \sum_{i,j=1}^N e^{i\mathbf{k} \cdot (\mathbf{r}_i - \mathbf{r}_j)} \right\rangle. \quad (\text{B3})$$

It is also instructive to examine the one-body density matrix $n(\mathbf{r})$, which measures the change in the wave function Ψ for a given particle displacement \mathbf{r} , or equivalently, the relative disturbance caused by inserting a test particle at a given distance from the origin. Like $g(\mathbf{r})$, the one-body density matrix depends only on the magnitude of r in the case of an infinite, homogeneous, isotropic system. It is readily estimated on the basis of its expression

$$n(\mathbf{r}) = \left\langle \frac{\Psi(\mathbf{r}_1, \mathbf{r}_2, \dots, \mathbf{r}_i + \mathbf{r}, \dots, \mathbf{r}_A)}{\Psi(\mathbf{r}_1, \mathbf{r}_2, \dots, \mathbf{r}_i, \dots, \mathbf{r}_A)} \right\rangle. \quad (\text{B4})$$

(For simplicity, we suppress spin variables.) This expected value is calculated by moving particle i , chosen at random

or systematically, by an amount \mathbf{r} and averaging the ratio of wave functions over an ensemble of configurations. The square of this ratio is computed at each stage of the walk, anyway, in implementing the Metropolis acceptance criterion. Consequently, very little extra cost is added to the energy calculation by binning the successive values for $n(\mathbf{r})$.

The Fourier transform of $n(\mathbf{r})$ is the probability density that a particle has a momentum \mathbf{k} . This momentum density $n(\mathbf{k})$ may be obtained in two ways. For the individual wave vectors contained within our simulation box we can compute $n(\mathbf{k})$ directly by performing the average

$$n(\mathbf{k}) = \left\langle e^{i\mathbf{k}\cdot\mathbf{r}} \frac{\Psi(\mathbf{r}_i + \mathbf{r})}{\Psi(\mathbf{r}_i)} \right\rangle. \quad (\text{B5})$$

Alternatively, a continuous $n(\mathbf{k})$ may be computed at the

end of the random walk by Fourier transforming the (appropriately smoothed) $n(\mathbf{r})$:

$$n(\mathbf{k}) = \rho \int e^{i\mathbf{k}\cdot\mathbf{r}} n(\mathbf{r}) d\mathbf{r}. \quad (\text{B6})$$

In practice, the numerical transforms of the MC data for $g(r) - 1$ and $n(r)$ do not yield very accurate representations of the respective functions $\rho^{-1}[S(k) - 1]$ and $n(k)$ corresponding to the given trial state. For efficiency, only the sphericalized versions of $g(r)$ and $n(r)$ are stored rather than $g(\mathbf{r})$ or $n(\mathbf{r})$, which are *not* spherically symmetric throughout the (finite) simulation volume. However, the operations of sphericalizing and Fourier transforming do not commute.¹⁹ Therefore, the preferred option is direct sampling of the momentum-dependent expectation values [viz., (B3) and (B5)] in the course of the random walk.

*Permanent address: Department of Physics, Washington University, St. Louis, MO 63130.

¹M. D. Miller and L. H. Nosanow, Phys. Rev. B **15**, 4376 (1977).

²E. Krotscheck, R. A. Smith, J. W. Clark, and R. M. Panoff, Phys. Rev. B **24**, 6383 (1981).

³J. W. Clark, Prog. Part. Nucl. Phys. **2**, 89 (1979).

⁴S. Rosati, in *From Particles to Nuclei*, Proceedings of the International School of Physics "Enrico Fermi," Course LXXIX, Varenna, 1981, edited by A. Molinari (North-Holland, Amsterdam, 1981).

⁵R. M. Panoff, J. W. Clark, M. A. Lee, K. E. Schmidt, M. H. Kalos, and G. V. Chester, Phys. Rev. Lett. **48**, 1675 (1982).

⁶M. F. Flynn, J. W. Clark, E. Krotscheck, R. A. Smith, and R. M. Panoff, Phys. Rev. B **32**, 2945 (1985).

⁷W. Kolos and L. Wolniewicz, J. Chem. Phys. **43**, 2429 (1965); Chem. Phys. Lett. **24**, 457 (1974).

⁸I. F. Silvera and J. T. M. Walraven, Phys. Rev. Lett. **44**, 164 (1980).

⁹B. W. Statt and A. J. Berlinsky, Phys. Rev. Lett. **45**, 2105 (1980).

¹⁰T. J. Greytak and D. Kleppner, in *New Trends in Atomic Physics*, Proceedings of the Les Houches Summer School of Theoretical Physics, Les Houches, 1982, edited by G. Greenberg and R. Stora (North-Holland, Amsterdam, 1984), p. 1125.

¹¹D. A. Bell, H. F. Hess, G. P. Kochanski, S. Buchman, L. Pollock, Y. M. Xiao, D. Kleppner, and T. J. Greytak, Phys. Rev. B **34**, 7670 (1986).

¹²D. Schiff and L. Verlet, Phys. Rev. **160**, 208 (1967).

¹³W. L. McMillan, Phys. Rev. **A138**, 442 (1965).

¹⁴V. R. Pandharipande and H. A. Bethe, Phys. Rev. C **7**, 1312 (1973).

¹⁵M. D. Miller (private communication).

¹⁶E. Manousakis, S. Fantoni, V. R. Pandharipande, and Q. N.

Usmani, Phys. Rev. B **28**, 3770 (1983).

¹⁷R. M. Panoff, K. E. Schmidt, M. H. Kalos, and G. V. Chester (unpublished).

¹⁸E. Krotscheck, in *Quantum Fluids and Solids*, Proceedings of the Symposium on Quantum Fluids and Solids, Sanibel Island, Florida, 1983, AIP Conf. Proc. No. 103, edited by E. D. Adams and G. G. Ihas (AIP, New York, 1983), p. 132.

¹⁹D. Ceperley, G. V. Chester, and M. H. Kalos, Phys. Rev. B **16**, 3081 (1977).

²⁰N. Metropolis, A. W. Rosenbluth, M. N. Rosenbluth, A. M. Teller, and E. Teller, J. Chem. Phys. **21**, 1087 (1953).

²¹K. E. Kürten and J. W. Clark, Phys. Rev. B **30**, 1342 (1984).

²²E. Krotscheck and R. A. Smith, Phys. Rev. B **27**, 4222 (1983).

²³E. Krotscheck and J. W. Clark, Nucl. Phys. **A328**, 73 (1979).

²⁴E. Krotscheck, J. W. Clark, and A. D. Jackson, Phys. Rev. B **28**, 5088 (1983).

²⁵K. E. Schmidt, M. H. Kalos, M. A. Lee, and G. V. Chester, Phys. Rev. Lett. **45**, 573 (1980).

²⁶K. E. Schmidt, M. A. Lee, M. H. Kalos, and G. V. Chester, Phys. Rev. Lett. **47**, 807 (1981).

²⁷D. Levesque and C. Lhuillier, Phys. Rev. B **21**, 5159 (1980).

²⁸R. P. Feynman and M. Cohen, Phys. Rev. **102**, 1189 (1956).

²⁹M. A. Lee, K. E. Schmidt, M. H. Kalos, and G. V. Chester, Phys. Rev. Lett. **46**, 728 (1981).

³⁰R. M. Panoff, in *Condensed Matter Theories II*, edited by P. Vashishta, R. K. Kalia, and R. F. Bishop (Plenum, New York, 1987).

³¹M. F. Flynn, Ph.D. thesis, Washington University, 1986 (unpublished).

³²M. L. Ristig and J. W. Clark, Phys. Rev. B **14**, 2875 (1976).

³³S. Fantoni, Nuovo Cimento A **44**, 191 (1978).

³⁴E. Krotscheck, Nucl. Phys. **A317**, 149 (1979).

³⁵H. W. Jackson and E. Feenberg, Ann. Phys. (N.Y.) **15**, 266 (1961).